Reduction of bright exciton lifetimes by radiation-induced disorder

Christopher N. Singh,[1] Xiang-Yang Liu,[1] Blas Pedro Uberuaga,[1] and Stephen J. Tobin[2]
[1]*Materials Science and Technology Division, Los Alamos National Laboratory, Los Alamos, New Mexico 87545, USA*
[2]*Detonator Science and Technology Division, Los Alamos National Laboratory, Los Alamos, New Mexico 87545, USA*

(Received 2 April 2021; revised 25 May 2021; accepted 25 June 2021; published 15 July 2021)

Quantum-radiative decay is a fundamental process in many optoelectronic systems such as laser diodes and solar cells. The bright exciton lifetime is a critical factor in determining the performance of these systems. Motivated by the ever-increasing need for laser systems in space and nuclear applications, we develop a many-particle approach to predict the radiative lifetime under harsh radiation environments. Using GaAs as a model system, we find that radiation-induced band tailing reduces the bright exciton lifetime. This result shows that the efficiency of radiative recombination, in addition to nonradiative recombination, can be affected by ionization radiation. Our approach enables a detailed understanding of the interplay between correlation, localization, and radiation that affect the performance of gain media.

DOI: 10.1103/PhysRevMaterials.5.073802

I. INTRODUCTION

Radiation-resilient optoelectronic materials are highly desired in space and nuclear applications [1,2], and knowing the radiative lifetimes of elementary excitations in these materials is crucial for both current and next-generation applications [3]. For example, intersatellite optical links, laser diodes, scintillators, and optical fiber-based communications are all exposed to different types, and fluences, of radiation as part of their normal operation [4]. Being able to predict the performance of these systems before they are deployed is a technical challenge because it requires bridging vast length scales and timescales [5]. In many of these applications, the component materials experience potentially damaging radiation fields that alter the atomic and electronic structure. In fact, microscopic light-matter interactions ultimately govern the macroscopic response of these devices, but the ability to quantitatively connect radiation damage with optical properties requires treating both fast electronic processes on the order of femtoseconds to nanoseconds and slow ionic processes that could develop over minutes, days, or even years [6]. Phenomenological solutions to this problem do exist [7–14], but recent developments in high-performance computing and first-principles approaches are beginning to enable direct simulation of these many length scales and timescales [5]. The challenge is to be able to connect changes in the ionic degrees of freedom (radiation-induced lattice disorder) to changes in the optoelectronic properties (many-particle radiative decay rates) with computationally tractable algorithms [15]. Because a dominant disorder-induced optical effect comes from band tailing [16,17], a general methodology to treat the electron-hole interaction in the presence of band tailing is highly desired.

Here, we develop a first-principles, many-body approach to treat disorder and correlation effects in radiation-damaged laser gain media. We find that radiation-induced changes to the electronic structure affect the radiative recombination efficiency by localizing exciton wave functions in the band edges. Our results show that the radiative recombination efficiency, in addition to the traditionally considered nonradiative recombination efficiency, is affected by radiation damage. This is a previously unappreciated leakage channel, and directly impacts the ability of a crystal gain medium to drive an optical resonator. This work is a crucial step in relating laser diode performance under harsh radiation conditions to the many-body radiative decay processes. It will enable different levels of predictive capability because many materials' optoelectronic properties are heavily influenced by disorder. For example, chemical disorder can impact lattice parameters and luminescence in multicomponent oxides, and vacancy disorder can introduce entirely different absorption bands in fused silica. In this sense, although the GaAs-based laser-gain media are used as a case study, the methodology developed here is applicable to other optical material systems susceptible to band-tailing effects such as light-emitting diodes (LEDs), solar cells, scintillators, etc. [18].

Band tailing in doped semiconductors refers to the existence of an exponential distribution of localized states inside the fundamental gap (see Fig. 1). These states occur at the band edges, and the origin of these states is a statistical distortion of the unperturbed crystal wave functions by random impurities and/or defects [19]. It is known that irradiation produces band tailing in semiconductors [20–22], and that band tailing can significantly affect stimulated emission [23,24]—one of the microscopic processes that govern diode light-conversion efficiency. Additionally, it is known that, of all the available heteroepitaxial layers in a laser diode, the quantum-well layer (the recombination layer) is the most affected by radiation-induced damage [25], and that this damage is proportional to the irradiation fluence [26]. These facts suggest that both radiative and nonradiative decay processes ought to be considered in the radiation resilience of optoelectronic systems. Consequently, we seek a first-principles method to understand the coupling between these factors. Ideally, a complete treatment of radiation-induced damage would account for changes in both the radiative and nonradiative decay channels simultaneously. Unfortunately,

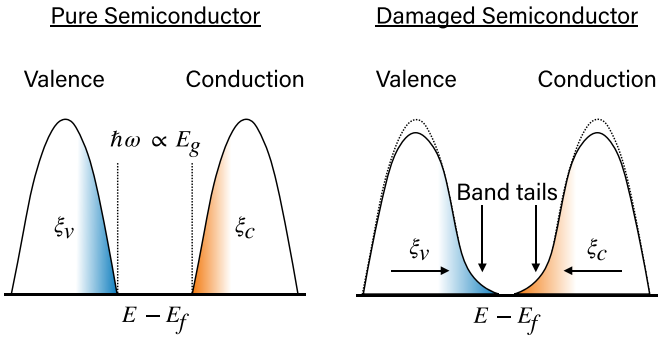

FIG. 1. Schematic representation of band-tailing effect and exciton weight redistribution. This figure shows the difference in the density of states between a pure semiconductor and a damaged one. The color indicates where the majority of the exciton weights are coming from. As radiation-induced damage to the electronic structure instantiates band tails, exciton weight is driven into the localized regions.

determining the nonradiative lifetime directly from first principles requires calculation of the electron-phonon matrix elements in the presence of disorder—a significant theoretical and computational challenge. Recent developments in the *ab initio* theory of electron-phonon coupling [27,28] may soon enable this type of calculation in defect systems, but at this time, it is beyond the scope of this work and we focus only on the radiative channel.

The primary degradation mechanism in laser diodes is a decrease in the minority carrier lifetime τ—it is commonly defined as $\tau^{-1} = \tau_r^{-1} + \tau_n^{-1}$, where τ_r is the radiative, and τ_n is the nonradiative component [26,29,30]. At equilibrium, the rate of injection, i.e., the current density J per unit length d, must equal the rate of change of carrier concentration qn/τ. Thus, if the radiative lifetime is too short, then large drive currents are necessary to achieve a population inversion (see Fig. 2). In fact, there is evidence that suggests the radiative rate can dominate the minority lifetime with certain defect concentrations [31]. If, on the other hand, the *nonradiative* lifetime is too short, then electron-hole pairs may preferentially decay via phonon—instead of photon—emission, decreasing the overall efficiency of the device. Figure 2 shows a typical band diagram of a lasing semiconductor heterostructure. As a bias is applied, quasichemical potentials for electrons and holes develop, driving electrons and holes into the recombination region. The rate of radiative decay (the bright exciton lifetime) inside the recombination region is a key parameter because it defines the rate at which injected carriers are converted into photons, and therefore, defines the current necessary to stabilize lasing.

II. METHODS

In order to calculate the radiative lifetime in the presence of radiation-induced lattice damage, we need (1) a high-fidelity model of the quantum-well electronic structure, (2) access to sufficient realizations of disorder, and (3) treatment of electron-hole and light-matter interactions. We use density functional theory (DFT) to obtain the electronic structure, perturbation theory to account for the light-matter interaction,

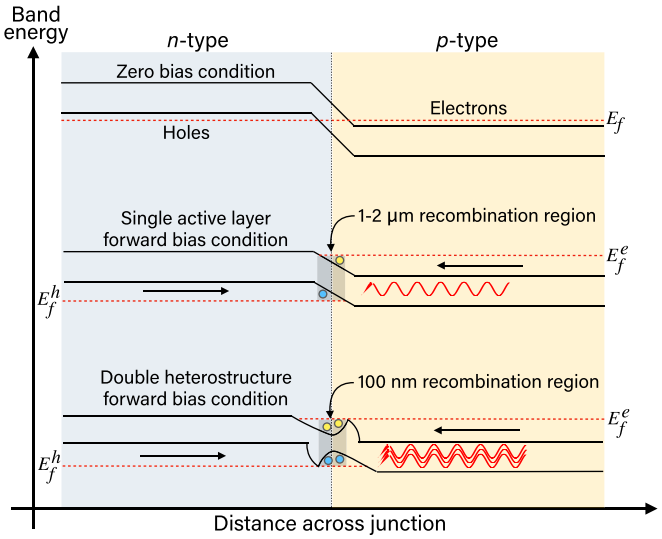

FIG. 2. Schematic band diagram of laser diode under various bias conditions. In the zero-bias condition, there is one chemical potential. Upon biasing, electrons and holes each have a quasichemical potential. In a multiple quantum-well heterostructure, the band offsets are used to drive electron-hole pairs into a smaller recombination region. In each case, the ability of the gain medium to store energy before converting it to light or heat is proportional to the electron-hole recombination time (bright exciton lifetime).

and the solution of the Bethe-Salpeter equation [32] (BSE) to account for the electron-hole interactions. A computationally efficient way to treat many realizations of disorder is to use the random potential method developed by Anderson [33]. Accordingly, the WIEN2K [34] and WANNIER90 [35] packages are used to generate the *ab initio* energy and position operator matrix elements: $\langle 0\alpha|H|\mathbf{R}\beta\rangle$ and $\langle 0\beta|\mathbf{r}|\mathbf{R}\alpha\rangle$, respectively. These will be used later to determine the dipole transition operator. A momentum space Hamiltonian on arbitrarily fine k meshes can then be defined for local orbitals α (β) as

$$H_{\alpha\beta}(\mathbf{k}) = \sum_{\mathbf{R}} \langle 0\alpha|H|\mathbf{R}\beta\rangle e^{i\mathbf{k}\cdot\mathbf{R}}. \quad (1)$$

The summation runs over N lattice translation vectors $\mathbf{R}$ corresponding to the number of unit cells considered in the calculation. The lattice defects caused by irradiation, e.g., atomic vacancies, substitutions, interstitials, etc., can be modeled as a perturbation Θ [33] of the undamaged electronic structure as

$$H^{\Theta}_{\alpha\beta}(\mathbf{k}) = \sum_{\mathbf{R}} \langle 0\alpha|H + \Theta(W)\delta_{\alpha\beta}\delta_{0\mathbf{R}}|\mathbf{R}\beta\rangle e^{i\mathbf{k}\cdot\mathbf{R}}. \quad (2)$$

The perturbation matrix elements Θ are random numbers pulled from a standard uniform distribution of width W centered at zero. Using this disorder potential has the advantage of producing band tailing in the electronic structure without having to run expensive molecular dynamics (MD) simulations or use large supercells, yet, reproduces the most salient features of several recent MD investigations [36–38]. Additionally, because there is an equal likelihood of creating electron or hole traps in this approach, it does not artificially shift the chemical potential. The stationarity of the chemical

potential under irradiation is in line with measurement [39]. Turning to the light-matter interaction, the canonical form is written as

$$H_{\rm int} = -\frac{e}{mc}\int d\mathbf{r}\ \Psi(\mathbf{r})^{\dagger}\mathbf{A}(\mathbf{r})\cdot\mathbf{p}\ \Psi(\mathbf{r}), \tag{3}$$

where $\mathbf{A}(\mathbf{r})$ is the electromagnetic vector potential, and $\mathbf{p}$ is the electron kinetic momentum. A quantized electromagnetic field is necessary to treat spontaneous emission, and therefore it is standard to expand the vector potential as plane waves [40]:

$$\mathbf{A}(\mathbf{r}) = \sum_{\mathbf{q}\lambda}\sqrt{\frac{2\pi\hbar c}{Vq}}\,\epsilon_{\mathbf{q}\lambda}[a^{\dagger}_{\mathbf{q}\lambda}e^{i\mathbf{q}\cdot\mathbf{r}} + \text{H.c.}]. \tag{4}$$

In Eq. (4), the boson operators $a^{\dagger}_{\mathbf{q}\lambda}$ create or destroy photons of momentum $\mathbf{q}$ and polarization $\epsilon_{\mathbf{q}\lambda}$ $-$ λ indexes the mode and H.c. indicates the Hermitian conjugate. The bright exciton lifetime τ_r is given by the inverse of the radiative decay rate Γ ($\tau_r = \Gamma^{-1}$). We follow Spataru *et al.* [41] and use Fermi's golden rule to write to the radiative decay rate as

$$\Gamma(\mathbf{Q}) = \frac{2\pi}{\hbar}\sum_{\mathbf{q}\lambda}|\langle G, 1_{\mathbf{q},\lambda}|H_{\rm int}|S(\mathbf{Q}),0\rangle|^2\delta(E_S(\mathbf{Q}) - \hbar c\mathbf{q}), \tag{5}$$

where $\mathbf{Q}$ is the exciton center of mass momentum, $\langle G, 1_{\mathbf{q},\lambda}|$ is a state with one photon and zero excitons, $|S(\mathbf{Q}),0\rangle$ is a state with zero photons and one exciton, and $E_S(\mathbf{Q})$ is the exciton energy defined by the eigenvalue equation

$$H_{\rm exc}|S(\mathbf{Q})\rangle = E_S|S(\mathbf{Q})\rangle. \tag{6}$$

The exciton Hamiltonian $H_{\rm exc}$ is written in a basis of electron-hole states following Wu *et al.* [42] as

$$\begin{aligned}&\langle v, c, \mathbf{k}, \mathbf{Q}|H_{\rm exc}|v', c', \mathbf{k}', \mathbf{Q}\rangle\\ &\quad= \delta_{vv'}\delta_{cc'}\delta_{\mathbf{k}\mathbf{k}'}(E_{(\mathbf{k}+\mathbf{Q})c} - E_{\mathbf{k}v}) - (D-X)^{cc'}_{vv'}(\mathbf{k},\mathbf{k}',\mathbf{Q}),\end{aligned} \tag{7}$$

where, unless otherwise stated, v and c index valence and conduction band states, E is the single-particle energy, and D and X are the direct and exchange two-particle matrix elements, respectively. They are defined as

$$D^{cc'}_{vv'}(\mathbf{k},\mathbf{k}',\mathbf{Q}) = V(\mathbf{k}-\mathbf{k}')\cdot(U^{\dagger}_{\mathbf{k}+\mathbf{Q}}U_{\mathbf{k}'+\mathbf{Q}})_{cc'}(U^{\dagger}_{\mathbf{k}'}U_{\mathbf{k}})_{v'v}, \tag{8a}$$

$$X^{cc'}_{vv'}(\mathbf{k},\mathbf{k}',\mathbf{Q}) = V(\mathbf{Q})\cdot(U^{\dagger}_{\mathbf{k}+\mathbf{Q}}U_{\mathbf{k}})_{cv}(U^{\dagger}_{\mathbf{k}'}U_{\mathbf{k}'+\mathbf{Q}})_{v'c'}, \tag{8b}$$

where U is the unitary matrix that diagonalizes $H^{\Theta}_{\alpha\beta}(\mathbf{k})$, and V is the interaction potential defined as [43,44]

$$V(\mathbf{k}-\mathbf{k}') = \frac{1}{N}\frac{4\pi e^2}{\varepsilon_0}\frac{1}{(\mathbf{k}-\mathbf{k}')\cdot(\mathbf{k}-\mathbf{k}')+\beta^2}, \tag{9a}$$

$$V(\mathbf{Q}) = \frac{1}{N}\frac{4\pi e^2}{\varepsilon_0}\frac{1}{\mathbf{Q}\cdot\mathbf{Q}+\beta^2}. \tag{9b}$$

Here, $\mathbf{k}$ is the crystal momentum, β is the inverse screening parameter, and N is the number of unit cells considered. Conservation of momentum forces the exciton center of mass momentum to equal the photon momentum $\mathbf{Q} = \mathbf{q}$, but the photon momentum is much less than the crystal momentum $|\mathbf{q}| \ll |\mathbf{k}|$. Therefore, we take the dielectric function as constant $\varepsilon(\mathbf{q}\to\mathbf{0}) \approx \varepsilon_0 \approx 8.9$ in GaAs [44]. Full *GW* calculations could in principle obtain the screened Coulomb interaction from first principles at the expense of computational simplicity. The exciton state is defined as a linear combination of electron-hole states:

$$|S(\mathbf{Q})\rangle = \sum_{vc\mathbf{k}} A^{S(\mathbf{Q})}_{vc\mathbf{k}} b^{\dagger}_{(\mathbf{k}+\mathbf{Q})c} b_{\mathbf{k}v}|GS\rangle. \tag{10}$$

Diagonalization of the exciton Hamiltonian $H_{\rm exc}$ [solution of Eq. (6)] gives the coefficients and energies needed to evaluate the matrix elements appearing in Eq. (5). These matrix elements can be expressed in terms of single-particle momentum matrix elements using Eqs. (4) and (10):

$$\begin{aligned}\langle G, 1_{\mathbf{q},\lambda}|H_{\rm int}|S(\mathbf{Q}),0\rangle = &-\frac{e}{mc}\sqrt{\frac{2\pi\hbar c}{Vq}}\,\epsilon_{\mathbf{q}\lambda}\\ &\cdot\sum_{vc\mathbf{k}} A^{S(\mathbf{Q})}_{vc\mathbf{k}}\langle v\mathbf{k}|e^{-i\mathbf{q}\cdot\mathbf{r}}\mathbf{p}|c\mathbf{k}+\mathbf{Q}\rangle.\end{aligned} \tag{11}$$

Here, $A^{S(\mathbf{Q})}_{vc\mathbf{k}}$ are coefficients of the exciton wave functions. Momentum conservation forces the exciton momentum to be equal to the photon momentum in three dimensions [45], and for optical photon energies, the matrix element on the right-hand side of Eq. (11) can be approximated in the Wannier basis as [46]

$$\begin{aligned}&\langle v\mathbf{k}|e^{-i\mathbf{q}\cdot\mathbf{r}}\mathbf{p}|c\mathbf{k}+\mathbf{Q}\rangle \approx \langle v\mathbf{k}|\mathbf{p}|c\mathbf{k}\rangle\delta_{\mathbf{q},\mathbf{Q}}\\ &\quad= i\sum_{\alpha\beta}U^{*}_{m\alpha}(\mathbf{k})U_{n\beta}(\mathbf{k})\sum_{\mathbf{R}}\langle 0\alpha|H|\mathbf{R}\beta\rangle\mathbf{R}e^{i\mathbf{k}\cdot\mathbf{R}}\\ &\qquad+ i\epsilon_m(\mathbf{k})\sum_{\alpha\beta}U^{*}_{m\alpha}(\mathbf{k})U_{n\beta}(\mathbf{k})\left(\sum_{\mathbf{R}}\langle 0\beta|\mathbf{r}|\mathbf{R}\alpha\rangle e^{i\mathbf{k}\cdot\mathbf{R}}\right)^{*}\\ &\qquad- i\epsilon_n(\mathbf{k})\sum_{\alpha\beta}U^{*}_{m\alpha}(\mathbf{k})U_{n\beta}(\mathbf{k})\sum_{\mathbf{R}}\langle 0\alpha|\mathbf{r}|\mathbf{R}\beta\rangle e^{i\mathbf{k}\cdot\mathbf{R}}.\end{aligned} \tag{12}$$

In the analysis presented above, the critical matrix elements $\langle 0\alpha|H|\mathbf{R}\beta\rangle$ and $\langle 0\alpha|\mathbf{r}|\mathbf{R}\beta\rangle$ are known from *ab initio* calculations. Therefore, Eqs. (6), (11), and (12) allow one to directly calculate the bright exciton lifetime in the presence of radiation damage using Eq. (5). In evaluating Eq. (5), we run the sum over two arbitrary polarizations λ, and $N_{\mathbf{q}}$ $\mathbf{q}$ points uniformly distributed on the surface of a sphere of radius $|E_0(\mathbf{0})/(hc)|$. The inverse screening parameter is fixed by setting $E_0(\mathbf{0})$ to approximate the experimental GaAs exciton binding energy (4.2 ± 0.3 meV) [47] for a given $\mathbf{k}$ mesh. We use a 0.7 Å^{-1} momentum space resolution. The lifetime predictions are averaged over 100 realizations of disorder.

The assumptions in the theory are the dipole approximation [Eq. (12)], and the assumption of homogeneous, Anderson-type disorder. Traditional methods [24,48] assume a constant matrix element and parabolic bands to determine the lifetime, but the approach given here relaxes both assumptions, and additionally accounts for two-particle matrix element effects. The dipole approximation is valid if the wavelength of the light field is far longer than the atomic dimension ($R_{\rm atom}/\lambda\!\!\!^{-} \sim Z/137 \ll 1$) [40]. This is an excellent approximation for many traditional gain media. Homogeneity of the damage across irradiation types is a weaker approximation because there are

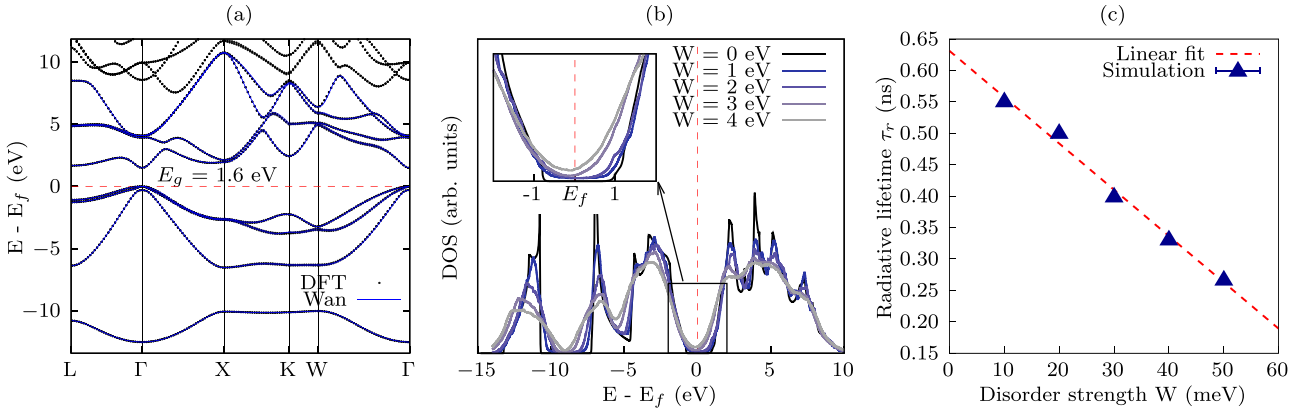

FIG. 3. Electronic structure and lifetime predictions of GaAs. (a) Compares the band structure predicted by DFT [modified Becke-Johnson (mBJ) functional] with the Wannier interpolation. (b) The density of states as a function of disorder strength W (eV). The inset shows a detailed view near the Fermi energy. The disorder strength is exaggerated for clarity. (c) The radiative lifetime τ_r as a function of disorder strength W. The points are the average over 100 disorder realizations.

conflicting reports in the literature about the exact nature of damage. For example, neutron irradiation has been shown to give a significant smearing of the absorption edge [22]. This is consistent with homogeneous disorder, but the effect of electron irradiation is less clear. Bourgoin and Angelis [49], and Hazra *et al.* [50] claim electron irradiation leads to uniform defects, while Stievenard *et al.* [51] claim it is anisotropic. In either case, Sagatova *et al.* [52] have shown that with the same impinging energy, gamma-ray effects are two orders of magnitude less than electron effects, which are one order of magnitude less than neutron effects. Regardless of the radiation type, however, enumerating possible defects and their effects on the electronic structure as a function of creation energy is possible with molecular dynamic and density functional techniques, and has been reported in several works [36–38]. A common behavior is the smearing of states into the gap from the band edges. Therefore, for the given computational cost, and for investigating changes in the electronic structure of 1–100 nm regions, we assume that band tailing is a reasonable approximation—again, in line with experimental evidence [53].

III. RESULTS AND DISCUSSION

Having laid out the formalism, we can now turn to the results. Figure 3 shows the electronic structure and lifetime predictions in GaAs. Figure 3(a) compares the band structure from density functional theory and from a Wannier interpolation [the eigenvalues of $H_{\alpha\beta}(\mathbf{k})$ from Eq. (1)]. In the energy range $-10 < E_f < +10$ eV, the difference between them is insignificant. This is evidence that the matrix elements $\langle 0\alpha|H|\mathbf{R}\beta\rangle$ and $\langle 0\beta|\mathbf{r}|\mathbf{R}\alpha\rangle$ accurately reflect an *ab initio* result. All eight valence orbitals are included in the Wannier basis. Spin-orbit coupling is also included. Therefore, there are 16 local degrees of freedom. Of the 16 available bands, two conduction and two valence bands are considered in the solution of the Bethe-Salpeter equation. Figure 3(b) shows the evolution of the density of states with increasing disorder strength W. We see that with increasing W, exponential tails develop at the band edges. This is the primary electronic effect we aimed to simulate, and Fig. 3(b) shows that the formalism is effective in this regard. Figure 3(c) is the main result, and shows the bright exciton lifetime as a function of disorder. We find the lifetime decreases linearly with increasing disorder, and that it is reduced by nearly a factor of 3 for the values studied here. This finding is in line with the expectation that the lifetime decreases proportional to the fluence of the radiation damaging the semiconductor, i.e., number of bombarding particles per square centimeter [26]. Our prediction of the radiative lifetime in bulk GaAs ($0.2 < \tau_r < 0.6$ ns) is in good agreement with existing reports (∼0.37 ns) [54–61], suggesting this approach could be of general utility to understand the influence of band tailing in other optoelectronic materials. Of course, the nonradiative lifetime plays a critical role here, and work is underway to enable direct determination of this quantity, but that is beyond the scope of this work.

In the context of laser diodes, a decrease in the radiative lifetime suggests an increase in the threshold current density. To see this, consider that the electron-hole population necessary to achieve gain is maintained only by the injected current. In equilibrium, the rate of change in this population is zero; equivalently, the rate that electron-hole pairs are created is equal to the rate that they are destroyed. Therefore, we can write $J = nqd/(\tau_r + \tau_n)$, where J is the current density, n is the electron-hole population, q is the elementary charge, and d is the thickness of the recombination region. Based on our own results and experimental results garnered from the literature, we assume that postirradiation lifetimes are linearly related to preirradiation lifetimes as $\tau_{r_f} = c_r\tau_{r_i}$, and $\tau_{n_f} = c_r\tau_{n_i}$ for the constants c_r and c_n. Then the ratio of the postirradiation threshold current density to the preirradiation threshold current density J_f/J_i can be written as a function of the constants c_r and c_n representing the radiative and nonradiative damage constants, respectively. Then

$$\delta J(c_r, c_n) = \frac{J_f}{J_i} = \frac{\tau_i}{\tau_f} = \frac{c_r\tau_{r_i} + c_n\tau_{n_i}}{c_r c_n(\tau_{r_i} + \tau_{n_i})}. \tag{13}$$

Equation (13) shows that, as the postirradiation lifetime decreases, the postirradiation threshold current increases. Because the internal quantum efficiency of bulk GaAs is ≈0.6–0.9, we can assume $\tau_n \approx 10\tau_r$. Within these assumptions, the postirradiation threshold current density could

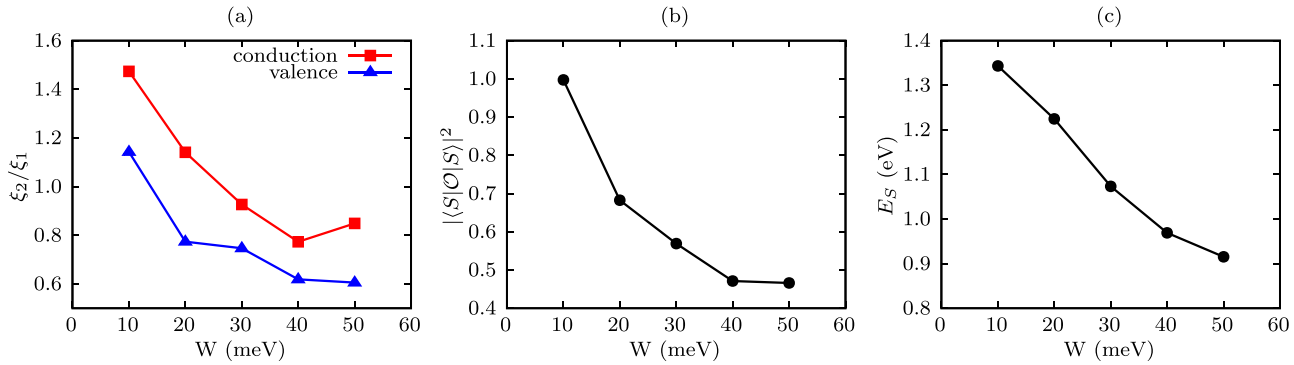

FIG. 4. Exciton characteristics as a function of disorder. (a) The ratio for the first and second valence band states normalized by the zero disorder ratio. (b) The overlap metric normalized by the zero disorder value. (c) The exciton energy. The lines are guides to the eye.

increase nearly fourfold, and that may be a significant change for certain applications. This analysis shows that we must put more energy per time into the system to maintain a threshold population with decreasing lifetime, and thus, band tailing in the gain medium has increased the energy necessary to reach the lasing threshold. We will show in Fig. 4 that this particular reduction in gain-medium efficiency is related to changes in the exciton wave function. We must stress, it is however likely that the nonradiative lifetime is not constant, and a complete understanding still requires knowledge of this variable as well. Until a first-principles approach to predict the nonradiative lifetime is available though, the method developed here can (in principle) be used in conjunction with laser delay measurements [62] to understand the evolution of nonradiative decay channels in irradiated systems.

Finally, in order to characterize the nature of the exciton wave functions in the valence and conduction band tails, we introduce the exciton weights

$$\xi_v^{S(\mathbf{Q})} = \frac{1}{N_\mathbf{k}} \sum_{c\mathbf{k}} \left|A_{vc\mathbf{k}}^{S(\mathbf{Q})}\right|^2, \tag{14a}$$

$$\xi_c^{S(\mathbf{Q})} = \frac{1}{N_\mathbf{k}} \sum_{v\mathbf{k}} \left|A_{vc\mathbf{k}}^{S(\mathbf{Q})}\right|^2. \tag{14b}$$

These weights represent the contribution of single-particle states to the exciton wave function. The ratio of the weights $(\xi_{v_2}^{S_1(0)}/\xi_{v_1}^{S_1(0)})$ as a function of disorder gives insight into how the weight shifts between bands during irradiation. Figure 4(a) plots the zero-disorder-normalized exciton weights for the first bright exciton ($S = 1$) as a function disorder strength. We find that with increasing disorder strength, the ratio decreases, meaning weight is driven into the localized band tails (recall Fig. 1 for a cartoon representation of this effect). Next, we also define an electron-hole overlap operator (in the transition basis) as

$$\mathcal{O}_{vv'}^{cc'}(\mathbf{k},\mathbf{k}',\mathbf{Q}) = (\mathbf{k}-\mathbf{k}')\cdot(\mathbf{k}-\mathbf{k}')(U_{\mathbf{k}+\mathbf{Q}}^\dagger U_{\mathbf{k}'+\mathbf{Q}})_{cc'}(U_{\mathbf{k}'}^\dagger U_\mathbf{k})_{v'v}. \tag{15}$$

The BSE ground-state expectation value of this operator $\langle S|\mathcal{O}|S\rangle$ will give insight into how the electron and hole overlap as a function of disorder. We find in Fig. 4(b) that with increasing disorder, the absolute square of this overlap metric decreases. A decline in electron-hole overlap is commensurate with the idea that localized electron and hole states now constitute the exciton. The surprising result is that the radiative lifetime also decreases. However, an inspection of Eqs. (5) and (11) will show there is a highly nonlinear relation between single-particle properties and the exciton lifetime. This is simply because the many-particle interaction matrix elements $\langle G, 1_{\mathbf{q},\lambda}|H_{\text{int}}|S(\mathbf{Q}),0\rangle$ depend on the exciton wave function and energies, and these are determined via eigendecomposition of the BSE. This brings us to Fig. 4(c). Figure 4(c) shows the BSE ground-state energy (exciton energy) as a function of disorder. We find a significant decrease due to the disorder-induced band tailing. These data together show the probability that electron-hole pairs occupy high-energy states is reduced, as most of the exciton weights are driven towards the gap. Because the exciton energy, electron-hole overlap, and radiative lifetime are all simultaneously reduced, this suggests that different damage effects are competing. For example, as band tails develop, the difference in energy between the single-particle electron and hole states is reduced. This makes decay more likely. But at the same time, a reduction in the spatial extent of the single-particle wave functions would reduce the Coulomb interaction between electrons and holes, making radiative decay less likely. Therefore, these two effects compete, and different materials with different gap sizes and susceptibility to forming band tails are expected to manifest this competition in a myriad of ways. In bulk GaAs, the change in energy seems to be dominant, but systems with larger fundamental gaps and less screening could behave differently. Changing the dimensionality of the system or the curvature of the bands could also play an important role.

IV. CONCLUSION

In summary, we have developed a many-body, first-principles approach to investigate the effect of radiation-induced lattice disorder that is applicable to a variety of important optoelectronic materials. We have shown that radiation-induced damage can fundamentally change the radiative decay processes by changing the character of the bright exciton wave functions. In the test case of bulk GaAs, these effects lead to a reduction of the radiative lifetime by approximately a factor of 3. Even if the nonradiative lifetime is approximately an order of magnitude greater than the radiative lifetime (as is typical), a factor-of-3 change in the radiative

component means the minority carrier lifetime will decrease by approximately two-thirds. Therefore, even the simplest analysis shows the approach developed here is important for understanding the relationship between radiation-induced disorder, radiative recombination, and optoelectronic efficiency. Further work is needed to investigate radiation-induced, nonradiative channels from first principles.

The data that support the findings of this study are available from the corresponding author upon reasonable request.

ACKNOWLEDGMENTS

This work was supported by Los Alamos National Laboratory. Los Alamos National Laboratory is operated by Triad National Security, LLC, for the National Nuclear Security Administration of the U.S. Department of Energy under Contract No. 89233218CNA000001. The authors would like to thank George Rodriguez, Mike Bowden, and Nate Sanchez for helpful discussions. A helpful interaction with Jian-Xin Zhu is also acknowledged.

[1] S. Girard, A. Morana, A. Ladaci, T. Robin, L. Mescia, J.-J. Bonnefois, M. Boutillier, J. Mekki, A. Paveau, B. Cadier, E. Marin, Y. Ouerdane, and A. Boukenter, J. Opt. **20**, 093001 (2018).

[2] H.-J. Kluge and W. Nörtershäuser, Spectrochim. Acta, Part B **58**, 1031 (2003).

[3] I. Aharonovich, D. Englund, and M. Toth, Nat. Photonics **10**, 631 (2016).

[4] J. R. Srour and J. M. McGarrity, Proc. IEEE **76**, 1443 (1988).

[5] K. Nordlund, J. Nucl. Mater. **520**, 273 (2019).

[6] K. Nordlund, S. J. Zinkle, A. E. Sand, F. Granberg, R. S. Averback, R. E. Stoller, T. Suzudo, L. Malerba, F. Banhart, W. J. Weber *et al.*, J. Nucl. Mater. **512**, 450 (2018).

[7] Y. Liu, S. Zhao, S. Yang, Y. Li, and R. Qiang, Microelectron. Reliab. **54**, 2735 (2014).

[8] O. Gilard, J. Appl. Phys. **93**, 1884 (2003).

[9] L. Smith, D. Wolford, R. Venkatasubramanian, and S. Ghandhi, MRS Online Proc. Libr. **163**, 95 (1989).

[10] D. Garbuzov, Czech. J. Phys. B **30**, 326 (1980).

[11] D. Garbuzov, J. Lumin. **27**, 109 (1982).

[12] H. Van Cong, J. Phys. Chem. Solids **42**, 95 (1981).

[13] V. Srinivas, J. Hryniewicz, Y. J. Chen, and C. E. C. Wood, Phys. Rev. B **46**, 10193 (1992).

[14] W. Bardyszewski and D. Yevick, Phys. Rev. B **39**, 10839 (1989).

[15] E. Y. Chen, C. Deo, and R. Dingreville, J. Phys.: Condens. Matter **32**, 045402 (2019).

[16] G. D. Cody, T. Tiedje, B. Abeles, B. Brooks, and Y. Goldstein, Phys. Rev. Lett. **47**, 1480 (1981).

[17] S. John, C. Soukoulis, M. H. Cohen, and E. N. Economou, Phys. Rev. Lett. **57**, 1777 (1986).

[18] J. C. Bourgoin and M. Zazoui, Semicond. Sci. Technol. **17**, 453 (2002).

[19] P. Van Mieghem, Rev. Mod. Phys. **64**, 755 (1992).

[20] A. Kalma, IEEE Trans. Nucl. Sci. **20**, 224 (1973).

[21] C. J. Hwang, Phys. Rev. B **6**, 1355 (1972).

[22] C. Barnes, J. Appl. Phys. **42**, 1941 (1971).

[23] F. Stern, Phys. Rev. **148**, 186 (1966).

[24] G. Lasher and F. Stern, Phys. Rev. **133**, A553 (1964).

[25] M. Boutillier, O. Gauthier-Lafaye, S. Bonnefont, F. Lozes-Dupuy, D. Lagarde, L. Lombez, X. Marie, V. Ligeret, O. Parillaud, M. Krakowski *et al.*, IEEE Trans. Nucl. Sci. **56**, 2155 (2009).

[26] B. Rose and C. Barnes, J. Appl. Phys. **53**, 1772 (1982).

[27] F. Giustino, Rev. Mod. Phys. **89**, 015003 (2017).

[28] F. Wu, T. J. Smart, J. Xu, and Y. Ping, Phys. Rev. B **100**, 081407(R) (2019).

[29] A. H. Johnston, IEEE Trans. Nucl. Sci. **50**, 689 (2003).

[30] S. L. Waterhouse and K. K. Jobbins, Radiation effects on laser diodes: a literary review, in *Proceedings of SPIE 7070, Optical Technologies for Arming, Safing, Fuzing, and Firing IV*, edited by Fred M. Dickey and Richard A. Beyer (SPIE, 2008), Vol. 70700E, pp. 123–132.

[31] G. B. Lush, H. F. MacMillan, B. M. Keyes, R. K. Ahrenkiel, M. R. Melloch, and M. S. Lundstrom, in *The Conference Record of the Twenty-Second IEEE Photovoltaic Specialists Conference - 1991* (IEEE, New York, 1991), Vol. 1, pp. 182–187.

[32] E. E. Salpeter and H. A. Bethe, Phys. Rev. **84**, 1232 (1951).

[33] P. W. Anderson, Phys. Rev. **109**, 1492 (1958).

[34] P. Blaha, K. Schwarz, G. K. H. Madsen, D. Kvasnicka, J. Luitz, R. Laskowski, F. Tran, and L. D. Marks, *WIEN2k, An Augmented Plane Wave + Local Orbitals Program for Calculating Crystal Properties* (Karlheinz Schwarz, Vienna University of Technology, Austria, 2018); J. Chem. Phys. **152**, 074101 (2020).

[35] G. Pizzi, V. Vitale, R. Arita, S. Blügel, F. Freimuth, G. Géranton, M. Gibertini, D. Gresch, C. Johnson, T. Koretsune *et al.*, J. Phys.: Condens. Matter **32**, 165902 (2020).

[36] M. Jiang, H. Xiao, S. Peng, G. Yang, Z. Liu, and X. Zu, Sci. Rep. **8**, 2012 (2018).

[37] M. Jiang, H. Xiao, S. Peng, L. Qiao, G. Yang, Z. Liu, and X. Zu, Nanoscale Res. Lett. **13**, 1 (2018).

[38] M. Jiang, H. Xiao, S. Peng, G. Yang, H. Gong, Z. Liu, L. Qiao, and X. Zu, J. Nucl. Mater. **516**, 228 (2019).

[39] D. Pons and J. Bourgoin, J. Phys. C **18**, 3839 (1985).

[40] J. J. Sakurai and E. D. Commins, *Modern Quantum Mechanics, Revised Edition* (Addison-Wesley, Reading, MA, 1995).

[41] C. D. Spataru, S. Ismail-Beigi, R. B. Capaz, and S. G. Louie, Phys. Rev. Lett. **95**, 247402 (2005).

[42] F. Wu, F. Qu, and A. H. MacDonald, Phys. Rev. B **91**, 075310 (2015).

[43] E. Kioupakis, D. Steiauf, P. Rinke, K. T. Delaney, and C. G. Van de Walle, Phys. Rev. B **92**, 035207 (2015).

[44] G. Cappellini, R. Del Sole, L. Reining, and F. Bechstedt, Phys. Rev. B **47**, 9892 (1993).

[45] H.-Y. Chen, V. A. Jhalani, M. Palummo, and M. Bernardi, Phys. Rev. B **100**, 075135 (2019).

[46] C.-C. Lee, Y.-T. Lee, M. Fukuda, and T. Ozaki, Phys. Rev. B **98**, 115115 (2018).

[47] S. B. Nam, D. C. Reynolds, C. W. Litton, R. J. Almassy, T. C. Collins, and C. M. Wolfe, Phys. Rev. B **13**, 761 (1976).

[48] N. K. Dutta, in *Semiconductors and Semimetals*, Vol. 39 (Elsevier, Amsterdam, 1993), pp. 1–38.

[49] J. Bourgoin and N. De Angelis, Sol. Energy Mater. Sol. Cells **66**, 467 (2001).

[50] P. Hazdra and S. Popelka, Mater. Sci. Forum **897**, 463 (2017).
[51] D. Stievenard, X. Boddaert, J. C. Bourgoin, and H. J. von Bardeleben, Phys. Rev. B **41**, 5271 (1990).
[52] A. Šagátová, B. Zat'ko, F. Dubecky, T. L. Anh, V. Nečas, K. Sedlačková, M. Pavlovič, and M. Fülöp, Appl. Surf. Sci. **395**, 66 (2017).
[53] N. Winogradoff and A. Neill, IEEE J. Quantum Electron. **4**, 111 (1968).
[54] M. Niemeyer, P. Kleinschmidt, A. W. Walker, L. E. Mundt, C. Timm, R. Lang, T. Hannappel, and D. Lackner, AIP Adv. **9**, 045034 (2019).
[55] G. Lush, Sol. Energy Mater. Sol. Cells **93**, 1225 (2009).
[56] H. Casey Jr and F. Stern, J. Appl. Phys. **47**, 631 (1976).
[57] P. J. Bishop, M. E. Daniels, B. K. Ridley, and K. Woodbridge, Phys. Rev. B **45**, 6686 (1992).
[58] R. Nelson and R. Sobers, J. Appl. Phys. **49**, 6103 (1978).
[59] R. Ahrenkiel, D. Dunlavy, B. Keyes, S. Vernon, T. Dixon, S. Tobin, K. Miller, and R. Hayes, Appl. Phys. Lett. **55**, 1088 (1989).
[60] F. Steranka, D. Defevere, S. Rudaz, D. Mc Elfresh, L. Cook, W. Snyder, M. Craford *et al.*, J. Electron. Mater. **24**, 1407 (1995).
[61] G. B. Lush, H. MacMillan, B. Keyes, D. Levi, M. R. Melloch, R. Ahrenkiel, and M. S. Lundstrom, J. Appl. Phys. **72**, 1436 (1992).
[62] G. W. 't Hooft, Appl. Phys. Lett. **39**, 389 (1981).